Nuclear and Thermal Analysis of a Multi-reflectometer System for DEMO

Yohanes Nietiadi[a], Raul Luís[a], Antonio Silva[a], Emanuel Ricardo[a], Bruno Gonçalves[a], Thomas Franke[b,c], Wolfgang Biel[d,e]

[a] *Instituto de Plasmas e Fusão Nuclear, Instituto Superior Técnico, Universidade de Lisboa, Av. Rovisco Pais 1, 1049-001 Lisboa, Portugal*
[b] *Max-Planck-Institut für Plasmaphysik, Garching, Germany*
[c] *EUROfusion Power Plant Physics and Technology (PPPT) department, Garching, Germany*
[d] *Institut für Energie und Klimaforschung, Forschungszentrum Jülich GmbH, Germany*
[e] *Department of Applied Physics, Ghent University, Belgium*

The reflectometry diagnostics for DEMO is envisaged to provide the radial edge density at several poloidal angles and data for the feedback control for plasma position and shape. The primary integration approach for reflectometry in DEMO involves the incorporation of several groups of antennas and waveguides into a diagnostics slim cassette (DSC), a full poloidal sector to be integrated with the water-cooled lithium lead (WCLL) breeding blanket. As the front-end components of the DSC will be directly exposed to the plasma, an effective cooling system is required. In this work, the temperature distributions of a DSC segment were estimated with a coupled steady-state thermal analysis performed with ANSYS Mechanical and ANSYS CFX, using the system-coupling module of ANSYS Workbench. The results, which also involved the computation of nuclear heat loads with MCNP6, indicate that the proposed cooling system design will lower the operation temperatures by more than 300 ºC when compared to previous designs. However, there will still be hotspots in some components, with temperatures above the limit of 550 °C for EUROFER under neutron irradiation.

Keywords: DEMO; Neutronics; Reflectometry; Diagnostics slim cassette; Thermal analysis

1. Introduction

Reflectometry measurements have been recently proposed for the next-generation fusion reactor DEMO as a suitable backup for magnetics sensors, the main tool for plasma behavior real-time monitoring [1]. The role of the reflectometry diagnostic in DEMO is twofold: i) to provide the radial edge density profile at several poloidal angles and ii) to provide data for the feedback control for plasma position and shape. The implementation of reflectometry requires that the antennas be placed in front of the plasma. As such, they are foreseen to be made of EUROFER, with the possible addition of tungsten coating, taken from the experience of the breeding blanket project for the use of materials for in-vessel components [2].

Ray-tracing simulations have shown that at the equatorial level the “single pair” approach for emitting and receiving antennas will be able to provide good spatial resolution. Near the lower and upper ports, however, the curvature of the plasma will cause significant problems for the operation and accuracy of reflectometry measurements. At these locations, a cluster of 4-6 antennas (3-5 per emitting antenna) may be required to ensure that the reflected beam is captured, even under conditions of larger plasma-wall distance. Therefore, to fulfill the reflectometry requirements, it is anticipated that up to 100 antennas will be required, distributed in 16 different poloidal locations [3].

The primary integration approach for reflectometry in DEMO has been based on the Diagnostics Slim Cassette (DSC) concept [4], a “dummy poloidal section” fully dedicated to diagnostics to be integrated with the Water-Cooled Lithium Lead (WCLL) Breeding Blankets (BB), illustrated in Figure 1 [4]. Since it is expected that several waveguides will go through each segment of DSC, a simple but effective cooling system design is mandatory to keep the operation temperatures under the maximum allowable operation temperature for EUROFER in DEMO (550°C) [5].

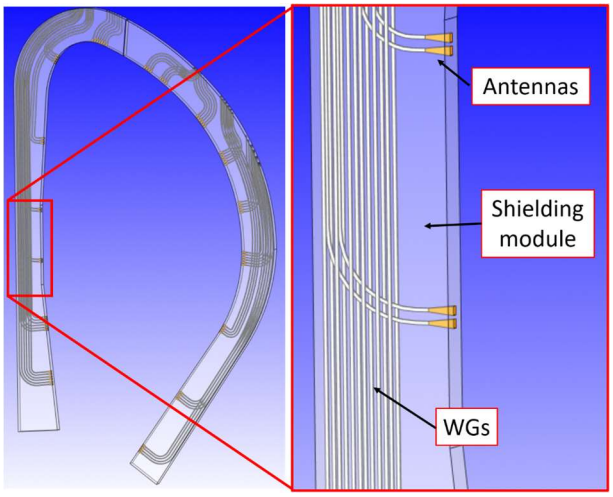

Figure 1: CAD representation of the reflectometry antennas and WGs in the DSC concept.

This paper presents the results of nuclear and thermal analysis performed for a new design of the DSC, using MCNP6 and ANSYS Workbench v19.1. A previous analysis [6] had shown that the highest heat loads in the antennas will be at the equatorial level; as such, the

author’s email: ynietiadi @ipfn.tecnico.ulisboa.pt

cooling system studied in this work was designed for a segment of the inboard module located at the equatorial plane.

2. Workflow and simulation tools

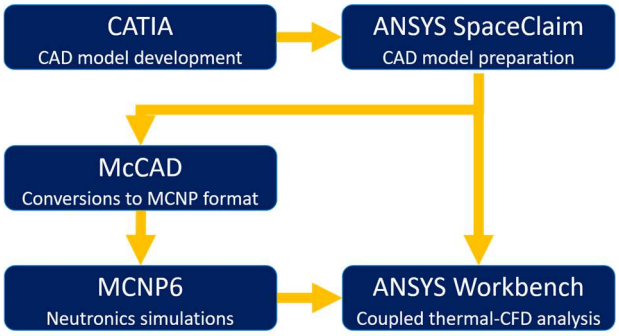

Figure 2: Workflow and simulation tools.

Figure 2 illustrates the steps followed to perform the simulations. The CAD software CATIA V5 [7] is used to develop the CAD models, which then must be imported to ANSYS SpaceClaim [8] for simplification – removal of fillets, screws, and other unnecessary complications – before they can be used in the nuclear and thermal analyses. For the nuclear analysis, the model is then decomposed as basic geometry, exported as STEP file and imported into the CAD-based modelling program McCad [9][10] for conversion to the MCNP input format. The neutronics simulations are performed in the Monte Carlo simulation program MCNP6 [11], after implementation of the converted model in a DEMO neutronics reference model, and the nuclear heat loads in the components of the DSC are then used as input in ANSYS Workbench v19.1[8] for the coupled thermal analysis (ANSYS Mechanical and CFD). The CAD models prepared in ANSYS SpaceClaim are used directly in the thermal analyses.

3. Inputs and assumptions

3.1 WG routing

As up to 100 antennas will be needed to fulfill the reflectometry requirements, one of the most important integration studies is to design the routing of the WGs inside the DSC for the new DEMO design introduced in 2017. For this purpose, input was taken from a previous work on the performance of reflectometry at 16 poloidal locations in the blanket, presented in [3].

A 20 cm wide (toroidal direction) DSC was designed, with the exact shape of the blankets, and clusters of pyramidal antennas were introduced in the first wall at the 16 locations. As more receiving antennas will be required to collect the reflected beams in gaps located further away from the equatorial plane, more antennas were introduced at these locations. In an iterative process, that aimed at using as much available space as possible, rectangular WGs were attached to the antennas and routed to the upper port. The main constraint, besides space, was the minimum radius of curvature required from reflectometry: 50 mm.

The DSC design is presented in Figure 3, which shows all the WGs on the left side and the WGs in different planes on the right side. The maximum number of antennas and WGs that could be introduced in the 20 cm wide SC was 73. Their implementation is shown in more detail in Figure 4; the antennas were distributed vertically around each gap and the clusters of antennas were distributed in different planes in the toroidal direction, to avoid clashing between WGs.

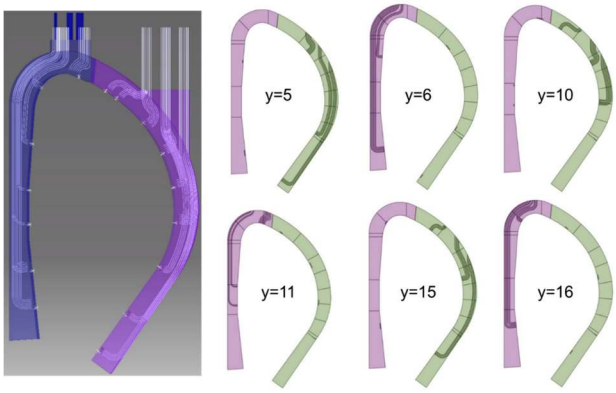

Figure 3: Routing of the maximum number of reflectometry WGs inside the DSC (y is the toroidal direction, units in cm).

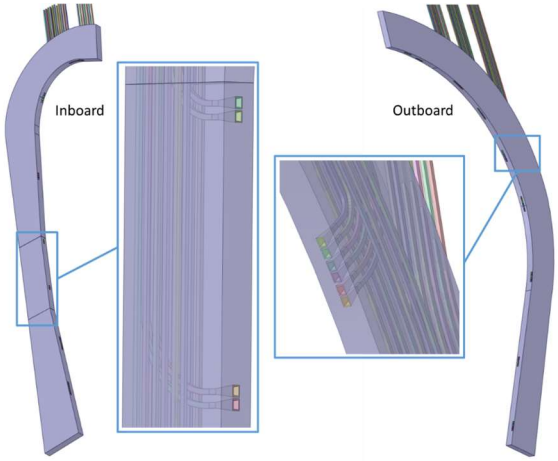

Figure 4: detail of the implementation of the antennas and WGs in the DSC.

3.2. CAD design of a DSC segment

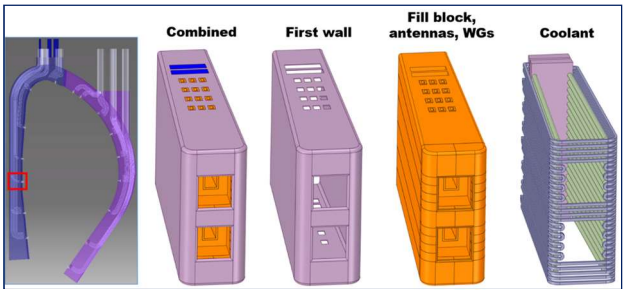

Figure 5: CAD model of a DSC segment at the equatorial plane (inboard).

As the performance of reflectometry at 16 poloidal locations is currently under study, the nuclear and thermal analyses presented here was carried out for a location that will have the antennas directed perpendicularly to the plasma, at the equatorial plane in the inboard side (Figure 5). To have the antennas recessed from the plasma, a 10-

cm cube was carved at the front of this module. Although in the current design this module has only one pair of antennas, the other 10 WGs that run through it were included in the design. The module is composed by the following components:

- A 2-mm tungsten layer on the outside (facing the plasma), with a dedicated cooling system;
- EUROFER components including the fill block (neutron shield / structural material), antennas and WGs;
- Water cooling system inside the fill block (water enters the system at 295°C, 15.5 MPa).

The most difficult challenge in the design of the DSC is to optimize the cooling system to bring the operation temperatures to acceptable values while keeping the design as simple as possible. This study took lessons from the design of the WCLL BB [12], to consider the integration aspects, and from the design of the Helium-Cooled Pebble Bed (HCPB) BB [13], which, like the DSC, has solid EUROFER as shielding material.

3.3. Nuclear analysis

For the nuclear analysis, the CAD model was decomposed and then converted to the MCNP input format using the CAD-based modelling program McCad. The result is presented in Figure 6 and Figure 7. This model was then implemented in the 22.5-degree 2017 Generic DEMO MCNP model [14], as shown in Figure 8. Using this model, neutronics simulations were performed to assess the nuclear loads in the system.

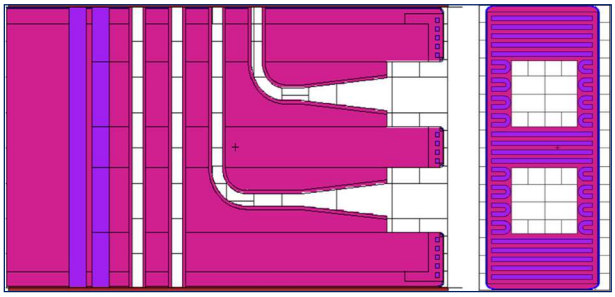

Figure 6: Poloidal (left) and front (right) planes of the MCNP model of the DSC.

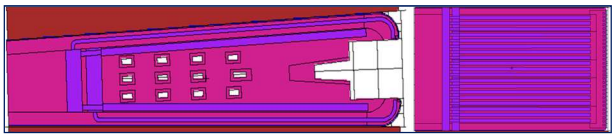

Figure 7: Toroidal (left) and poloidal (right) planes of the MCNP model of the DSC.

The MCNP simulations were run with mode N P to simulate the transport of neutrons and gammas, using FENDL 3.1 cross sections [15]. The results were normalized to a fusion power of 2037 MW. To keep the statistical errors below 10% and to ensure that all tallies pass the 10 statistical tests of MCNP, 2E9 source particles were simulated. A very fine mesh with 750000 bins (7.8mm x 2.8mm x 4.4mm) was defined to calculate the nuclear heat loads in the DSC module, to be used as input in the thermal analysis.

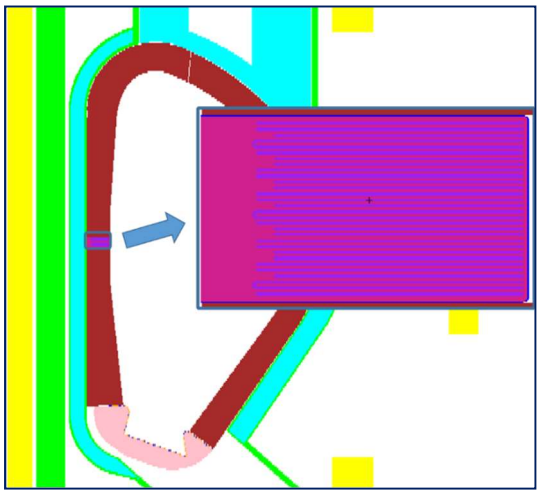

Figure 8: Poloidal view of the DSC integration in the MCNP reference model.

3.4. Coupled thermal analysis

3.4.1 Thermal radiation from the plasma

The thermal radiation from the plasma can be calculated using ANSYS CFX, by modelling the vacuum region between the plasma surface and the DSC as a fluid domain (Figure 9). The fluid domain is modelled using the properties of ideal gas for air at a pressure of 1E-10 Torr. The other boundary conditions for this calculation are:

- Power density of 500kW/m^2 at the plasma surface;
- Surface-to-surface Discrete Transfer Model (Shah model [16]) for the radiation phenomena, to take into account the direction of the radiation receiving surfaces;
- Emissivity of the plasma surface and the DSC surfaces set to 1 (Black-body radiation);
- All the surfaces of the fluid domain assumed to be adiabatic (the only heat transfer mechanism is by radiation).

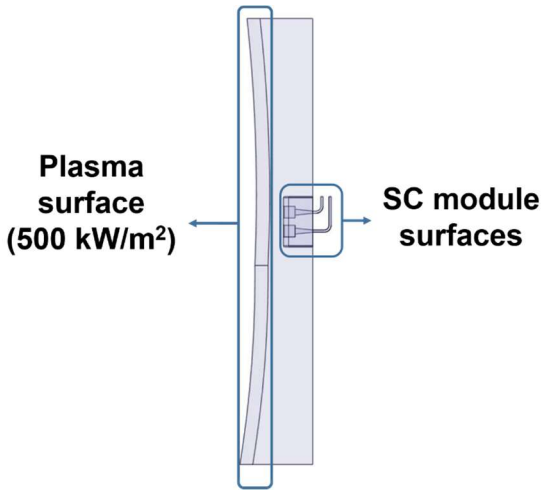

Figure 9: Modelling the thermal radiation from the plasma.

3.4.2 Steady-state thermal analysis setup for the solid elements

To reduce the computational time of each simulation, the thermal analysis of the solid elements was performed using the steady-state thermal analysis module of ANSYS Mechanical, since ANSYS Mechanical can make use of the GPU accelerator and CFX does not support this feature. The geometry used for this analysis consisted of the solid parts of the geometry shown in Figure 5 (tungsten cover, fill blocks, antennas, and waveguides). The temperature-dependent thermo-physical properties of the materials (EUROFER and tungsten) were taken from the WCLL blanket design [17] and are presented in Table 1 and Table 2.

Table 1: Thermo-physical properties of EUROFER [17].

T(°C)	*ρ (kg/m³)*	*C_p (J kg⁻¹ K⁻¹)*	*λ (W m⁻¹ K⁻¹)*
20	7750	448	28.3
100	7728	486	29.2
200	7699	522	30.7
250		537	
300	7666	551	30.2
350		566	
400	7633	584	29.3
450		612	
500	7596	655	29.5
550		721	
600	7558	801	31.2

Table 2: Thermo-physical properties of Tungsten [17].

T(°C)	*ρ (kg/m³)*	*C_p (J kg⁻¹ K⁻¹)*	*λ (W m⁻¹ K⁻¹)*
20	19298	129.0	172.8
100	19279	131.6	164.8
200	19254	134.7	155.5
300	19229	137.8	147.2
400	19205	140.9	139.8
500	19178	143.9	133.1
600	19152	146.8	127.2
700	19125	149.6	122.1

The nuclear heat loads (input from the nuclear analysis described in previous section) were imported as internal heat generation in all the solid elements, and the plasma thermal radiation was defined as heat flux to the plasma-facing surfaces.

The other boundary conditions were:

- Fluid-solid interface (FSI) definition for all solid surfaces interacting with the coolant;
- Constant temperature of 400°C in both sides of the module (assuming contact with the WCLL BB);
- Thermal radiation with emissivity of 0.5 in the front surfaces of the system;
- Adiabatic boundary condition for all the remaining surfaces.

3.4.3 Steady-state CFD analysis setup for the water coolant

Since the fluid domain does not interact directly with the plasma, the thermal load for the fluid domain is just the nuclear heat load, imported as internal heat generation, and the heat on the walls of the cooling channels, modelled with system coupling between ANSYS Mechanical and ANSYS CFX. The operation pressure and the static temperature of the water coolant are set to PWR conditions (295°C, 15.5 MPa for the inlet). The corresponding temperature-dependent thermo-physical properties of water, shown in Table 3, were imported and applied as a function of the operation temperature using profile data tools.

Table 3: Thermo-physical properties of water[17].

T(°C)	*ρ (kg/m³)*	*C_p (J kg⁻¹ K⁻¹)*	*λ (W m⁻¹ K⁻¹)*	*μ (10⁻⁶ kg m⁻¹ s⁻¹)*
200	875	4404	0.676	137.0
210	863	4443	0.670	130.0
220	852	4489	0.662	124.0
230	839	4542	0.653	119.0
240	825	4606	0.643	114.0
250	812	4684	0.633	110.0
260	797	4778	0.621	106.0
270	782	4895	0.607	102.0
280	765	5043	0.593	98.2
290	747	5232	0.577	94.9
300	727	5481	0.559	91.7
310	705	5818	0.539	88.3
320	680	6290	0.516	84.5

The other boundary conditions were:

- Adiabatic condition applied to the walls;
- Inlet mass flow rate and outlet static pressure at flow domain inlet and outlet sections;
- No-slip condition at the interface between coolant and the EUROFER cooling channels;
- Reynold Averaged Navier-Stokes (RANS) equations, two-equation k-ω Shear Stress Transport (SST) model employed to simulate the turbulence effects;
- Buoyancy effect modelled by setting the gravity on the z-direction as -9.8 m/s^2.

3.4.4 System coupling setup

The system coupling module of ANSYS Workbench was used to couple the thermal analysis of the solid elements and the CFD analysis through the fluid-solid interface. With this module, the total forces and heat fluxes are conservative across the FSI interface and information is sent both ways until the solution converges for both the solid steady-state thermal and the steady-state CFD analysis. The information sent from the solid steady-state thermal analysis is the cooling channel wall temperature, while the film heat transfer coefficient and the coolant temperature are sent from the CFD simulation to the solid steady-state thermal analysis as feedback.

4. Results and discussion

4.1 Nuclear analysis

Figure 10 and Figure 11 show the neuron and gamma fluxes in the DSC module, while the nuclear heat loads are presented in the same poloidal plane in Figure 12 and at the first wall circuit in Figure 13. As expected, the nuclear heat loads by neutrons are much higher in the water than in EUROFER, while the heat loads by gammas are higher in EUROFER and lower in water. When both are summed, there is not a sizable difference between the total heat loads in EUROFER and water. These nuclear heat loads were used as input in the thermal analysis.

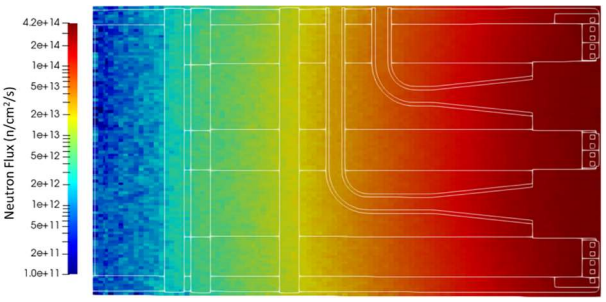

Figure 10: Neutron fluxes (n/cm^2/s) in the DSC module.

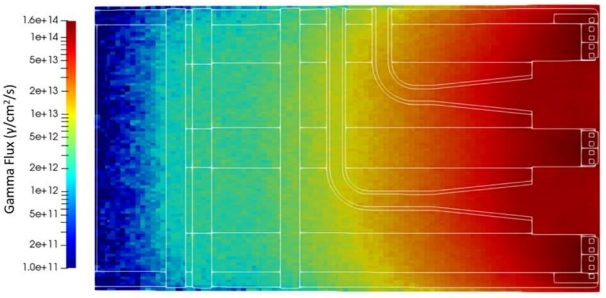

Figure 11: Gamma fluxes (γ/cm^2/s) in the DSC module.

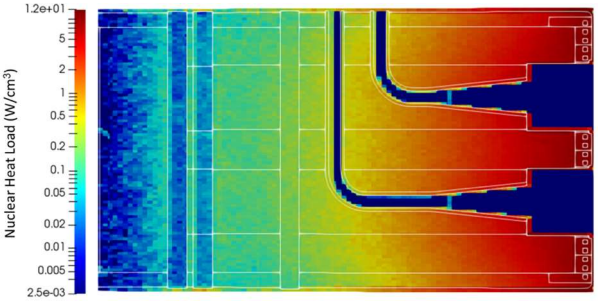

Figure 12: Nuclear heat loads (W/cm^3) in the DSC module.

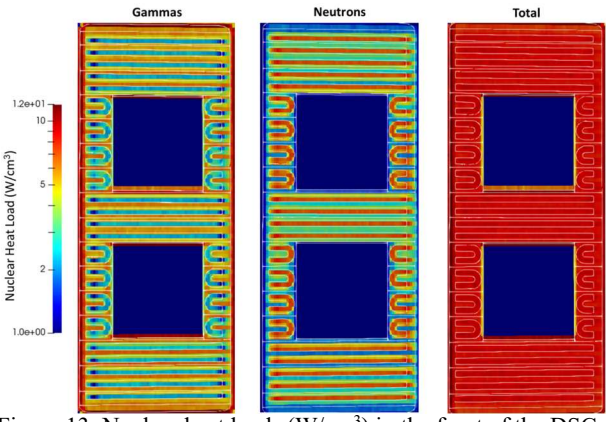

Figure 13: Nuclear heat loads (W/cm^3) in the front of the DSC module.

4.2 Plasma thermal radiation

From this calculation, a maximum heat flux of 316kW/m^2 was obtained, as presented in Figure 14. To improve the clarity, a narrower scale is provided on the right, which shows the effectiveness of the 10-cm cube carved in the first wall to reduce the thermal loads on the antennas.

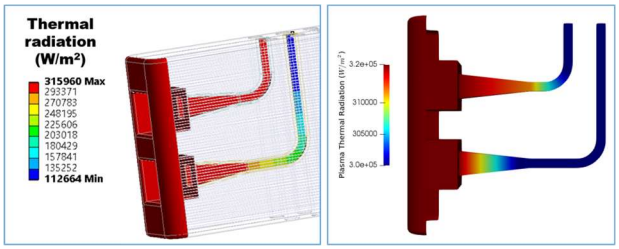

Figure 14: Thermal radiation from the plasma to the DSC surfaces. Left: ANSYS output. Right: same results plotted with a narrower scale using Paraview [18][19].

4.3 Coupled thermal-CFD analysis

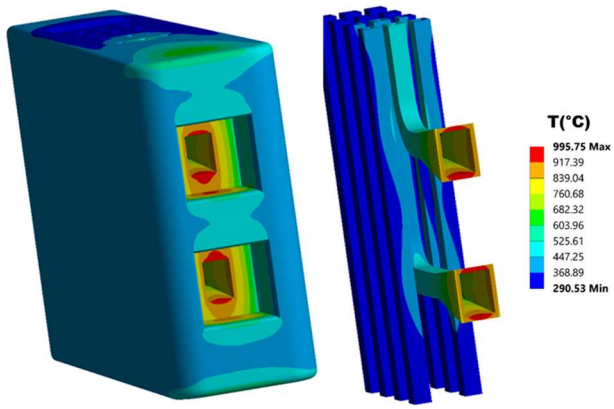

Figure 15: Temperature distribution (°C) in the current design of DSC module.

The operation temperatures obtained with the current design of DSC module are presented in Figure 15. The maximum temperature is 996°C, obtained at the tips of the reflectometry antennas and on the walls that surround them. This is because the edges of the antennas are sharp and located too far away from the shielding block cooling channels. The temperatures in the first wall, on the other hand, are much lower, below 500°C in most of the module except the hotspots at the top and bottom part, which

nevertheless have temperatures more than 300°C lower than the antennas. In these simulations, the water flow rate was optimized to ensure that its maximum temperature does not reach the boiling point of water at 15.5 MPa (344.79°C). Figure 16 shows that the maximum temperature in water, obtained for the first wall cooling circuit, is below 342.4°C. This is achieved with a total mass flow rate of 4.59 kg/s in the DSC inlet. In the fill blocks cooling system, the water temperature is always below 320°C.

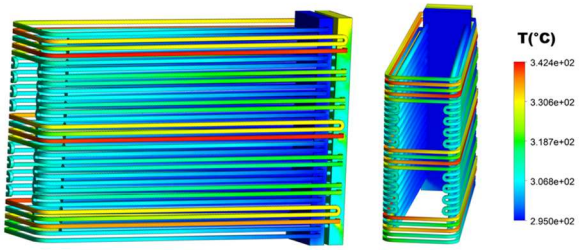

Figure 16: Temperature distribution (°C) in the water coolant.

4.4 Updated design

The results show that the operation temperature of the current DSC design is way above the maximum allowable temperature for EUROFER under irradiation environment. Therefore, a new design of the cooling system is required, with the aim to remove the hotspots presented in Figure 15. This can be achieved by moving the fill block cooling channels closer to the hotspots while adjusting the length of each cooling channel to follow the DSC first wall topology. To do this, the position of the cooling channels was changed in the toroidal direction, so that in the new design the cooling channels are inserted between the waveguide rows, as shown in Figure 17 and Figure 18.

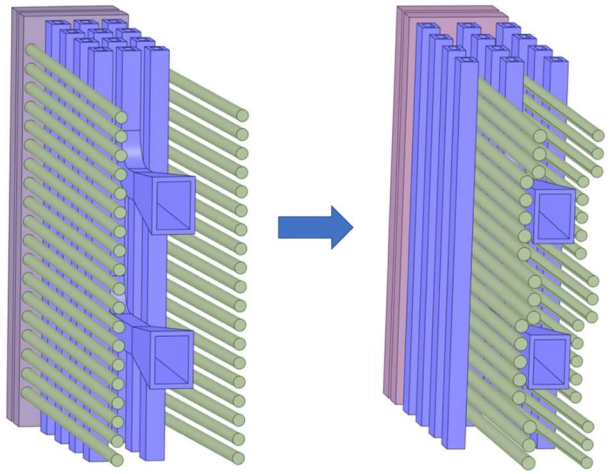

Figure 17: Updated design of the fill block cooling system.

After the change in the fill block cooling system design, a new MCNP model was created and the nuclear heat loads were recalculated, as shown in Figure 19. The thermal radiation from the plasma and the remaining boundary conditions, including the coolant inlet total mass flow rate, were kept unchanged, as they are not affected by the new design. In the updated thermal analysis, the maximum temperature obtained in the DSC module was 656°C, as illustrated in Figure 20 and Figure 21. Figure 22 shows that the temperature of water in the cooling channels remains below the boiling point.

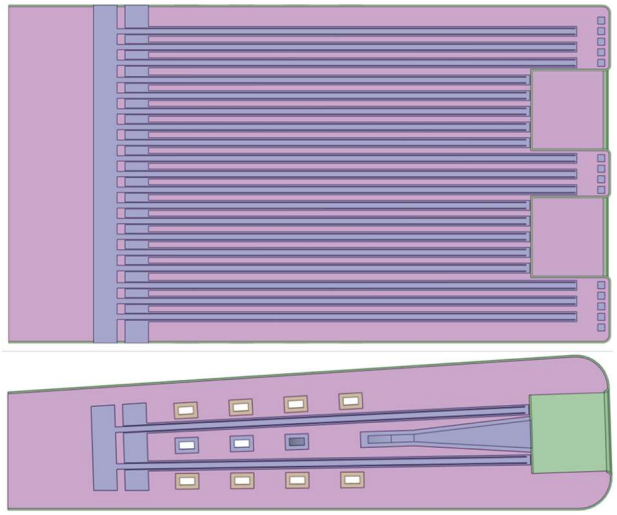

Figure 18: Detail of the updated design for the shielding blocks cooling system.

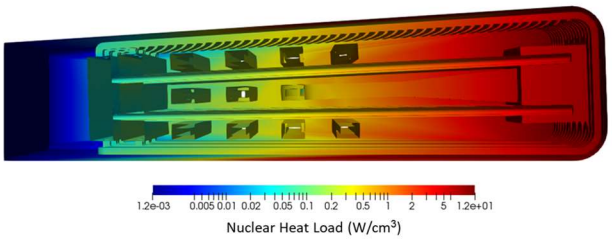

Figure 19: Total nuclear heat loads (W/cm^3) in the updated design of DSC module.

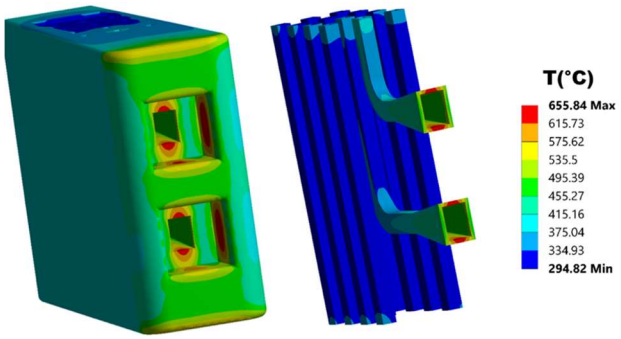

Figure 20: Temperature distribution (°C) in the DSC module: plasma-facing surface(left) and antennas and WGs (right).

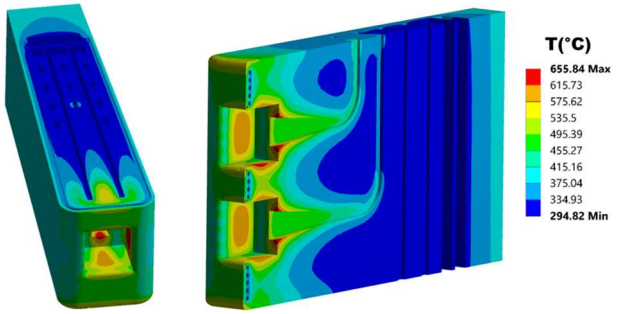

Figure 21: Temperature distribution (°C) in the DSC module: toroidal (left) and poloidal (right) cuts.

The maximum temperature obtained with the new configuration is more than 300°C lower than in the previous case, which shows the effectiveness of the updated design to lower the operation temperatures close

to the antennas. Furthermore, it is only ~30°C higher than the maximum temperature obtained in EUROFER in the thermal analyses of the HCPB BB [20]. It is also important to notice that steady-state thermal and CFD analyses like the one presented here lead to conservative estimations, when compared to the more realistic transient ones.

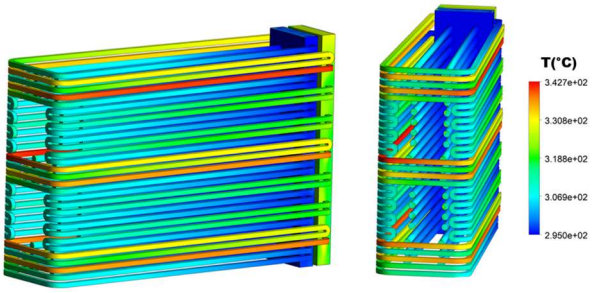

Figure 22: Temperature distribution (°C) in the updated cooling system.

4. Conclusions

In this work, we presented a new design of the Diagnostics Slim Cassette (DSC), currently proposed in DEMO for the integration of reflectometry antennas and waveguides with the DEMO WCLL breeding blankets. A 20-cm thick full poloidal sector was designed, with the exact shape of the blankets, and clusters of pyramidal antennas (73 in total, due to space constraints) were introduced in the first wall at 16 locations. In an iterative design process, that aimed at using as much available space as possible, rectangular WGs were attached to the antennas and routed to the upper ports.

From this design, one segment at the equatorial plane inboard was studied in detail, and a preliminary cooling system was developed. Nuclear and thermal analyses were performed for this segment, using MCNP6, ANSYS Mechanical and ANSYS CFX. Results show that the direct exposure to intense neutron and gamma fluxes, as well as the thermal radiation from the plasma, creates hotspots in the proposed design, mostly in the regions located further away from the cooling channels, such as the tips of the antennas and the walls surrounding them.

The next design iteration consisted in alternating the two rows of the fill block cooling channels with the three rows of waveguides, so that the cooling channels can get closer to the hotspots. In the thermal analysis performed with this design, the maximum temperature obtained in the SC module was 656 °C, more than 300 °C lower than in the previous case and only ~30°C higher than the maximum temperature obtained for EUROFER in the thermal analysis of the HCPB breeding blanket. This shows the effectiveness of the updated design to lower the operation temperatures close to the antennas. Nevertheless, there are still hotspots with temperatures above the limit for EUROFER under neutron irradiation. It is expected that micro-optimizations to the configuration of the cooling pipes will lead to a further decrease of the maximum temperature close to the antennas. For this, detailed sensitivity studies and a preliminary structural analysis shall be performed in the near future.

Acknowledgments

This work has been carried out within the framework of the EUROfusion Consortium and has received funding from the Euratom research and training programme 2014-2018 and 2019-2020 under grant agreement No. 633053. The reviews and opinions expressed herein do not necessarily reflect those of the European Commission. IST activities also received financial support from Fundação para a Ciência e Tecnologia (FCT) through the individual grant PD/BD/135230/2017 under the APPLAuSE Doctoral Program.

References

[1] W. Biel et al., *Diagnostics for plasma control – From ITER to DEMO*, Fus. Engin. Des. **146** (2019) 465–472

[2] G. Federici et al., *An overview of the EU breeding blanket design strategy as an integral part of the DEMO design effort*, Fus. Engin. Des. **141** (2019) 30-42.

[3] E. Ricardo et al., *Assessment of a multi-reflectometers positioning system for DEMO plasmas*, Journal of Instrumentation **14** (2019) C08010.

[4] A. Malaquias et al., *Integration Concept of the Reflectometry Diagnostics for the Main Plasma in DEMO*, IEEE Transactions on Plasma Science **46-2** (2018) 451-457

[5] R. Lässer et al., *Strucutral materials for DEMO: The EU development, strategy, testing and modelling*, Fus. Engin. Des. **82** (2007) 511-520.

[6] R. Luís et al., *Nuclear and Thermal Analysis of a Reflectometry Diagnostics Concept for DEMO*, IEEE Transactions on Plasma Science **46-5** (2018) 1247-1253.

[7] *CATIA® V5*, Dassault Systèmes, Release 6R2018

[8] ANSYS® Academic Research, Release 19.1

[9] B. Weinhorst et al., *Comparative assessment of different approaches for the use of CAD geometry in Monte Carlo transport calculations*, Fus. Engin. Des. **98-99** (2015) 2094-2097

[10] L. Lu, Y. Qiu, and U. Fischer, *Improved solid decomposition algorithm for the CAD-to-MC conversion tool McCad*, Fus. Engin. Des. **124** (2017) 1269-1272

[11] J.T. Goorley, et al., Initial MCNP6 Release Overview - MCNP6 Version 1.0, (2013)

[12] A. Del Nevo et al., *WCLL breeding blanket design and integration for DEMO 2015: status and perspectives*, Fus. Engin. Des. **124** (2017) 682-686

[13] F. Hernandez et al., *A new HCPB breeding blanket for the EU DEMO: Evolution, rationale and preliminary performances*, Fus. Engin. Des. **124** (2017) 882-886

[14] D. Flammini, 2017 Generic DEMO MCNP model at 22.5 degree v1.3 (2019)

[15] FENDL-3.1d: Fusion Evaluated Nuclear Data Library ver.3.1d, (2018) https://wwwnds.iaea.org/fendl/

[16] F. C. Lockwood, N. G. Shah, *A new radiation solution method for incorporation in general combustion prediction procedures*, Proc. 18th Int. Symp. on Combustion, The Combustion Institute, Pittsburgh, PA, p. 1405–1413 (1981).

[17] A. Del Nevo et al. WCLL design report 2017, Eurofusion

IDM reference: EFDA_D_2MYHNE v1.1, 2017
[18] J. Ahrens et al., *Paraview: An End-User Tool for Large Data Visualization, Visualization Handbook*, Elsevier, 2005, ISBN-13: 978-0123875822
[19] U. Ayachit, The Paraview Guide: A Parallel Visualization Application, Kitware, 2015, ISBN 978-1930934306
[20] F. Hernández et al. HCPB Design Report 2017, Eurofusion IDM reference: EFDA_D_2N66T5 v1.0, 2017